Hydrological Sciences Journal

ISSN: 0262-6667 (Print) 2150-3435 (Online) Journal homepage: http://www.tandfonline.com/loi/thsj20

Development of an operational low-flow index for hydrological drought monitoring over Europe

Carmelo Cammalleri, Jürgen Vogt & Peter Salamon

To cite this article: Carmelo Cammalleri, Jürgen Vogt & Peter Salamon (2016): Development of an operational low-flow index for hydrological drought monitoring over Europe, Hydrological Sciences Journal, DOI: 10.1080/02626667.2016.1240869

To link to this article: http://dx.doi.org/10.1080/02626667.2016.1240869

Accepted author version posted online: 06 Oct 2016.
Published online: 24 Oct 2016.

HYDROLOGICAL SCIENCES JOURNAL – JOURNAL DES SCIENCES HYDROLOGIQUES, 2016
http://dx.doi.org/10.1080/02626667.2016.1240869

Development of an operational low-flow index for hydrological drought monitoring over Europe

Carmelo Cammalleri, Jürgen Vogt and Peter Salamon

European Commission, Joint Research Centre (JRC), Ispra, VA, Italy

ABSTRACT

Near real-time monitoring of hydrological drought requires the implementation of an index capable of capturing the dynamic nature of the phenomenon. Starting from a dataset of modelled daily streamflow data, a low-flow index was developed based on the total water deficit of the discharge values below a certain threshold. In order to account for a range of hydrological regimes, a daily 95th percentile threshold was adopted, which was computed by means of a 31-day moving window. The observed historical total water deficits were statistically fitted by means of the exponential distribution and the corresponding probability values were used as a measure of hydrological drought severity. This approach has the advantage that it directly exploits daily streamflow values, as well as allowing a near real-time update of the index at regular time steps (i.e. 10 days, or dekad). The proposed approach was implemented on discharge data simulated by the LISFLOOD model over Europe during the period 1995–2015; its reliability was tested on four case studies found within the European drought reference database, as well as against the most recent summer drought observed in Central Europe in 2015. These validations, even if only qualitative, highlighted the ability of the index to capture the timing (starting date and duration) of the main historical hydrological drought events, and its good performance in comparison with the commonly used standardized runoff index (SRI). Additionally, the spatial evolution of the most recent event was captured well in a simulated near real-time test case, suggesting the suitability of the index for operational implementation within the European Drought Observatory.

ARTICLE HISTORY
Received 25 September 2015
Accepted 14 July 2016

EDITOR
M.C. Acreman

ASSOCIATE EDITOR
G. Di Baldassarre

KEYWORDS
Streamflow drought; European Drought Observatory (EDO); LISFLOOD model

1 Introduction

Drought is considered one of the major natural hazards due to its severe environmental, agricultural, health, economic and social consequences. It is commonly seen as a recurring phenomenon in various parts of the world, and over Europe an increase in the frequency, duration and intensity of droughts and related impacts has been observed over the past decades (European Commission 2007, Spinoni *et al.* 2015). The Joint Research Centre (JRC) of the European Commission has focused on integrating various drought information over continental Europe, resulting in the European Drought Observatory (EDO, http://edo.jrc.ec.europa.eu); this system aims to incorporate a wide range of indicators due to the complexity of the drought phenomenon.

By defining drought as an extended period when a region is affected by a deficiency in water supply, the characteristics of the drought, as well as the sectors impacted (e.g. agriculture, forestry, energy, transport), may differ greatly depending on the phase of the hydrological cycle interested by this deficit (e.g. precipitation, evaporation, runoff). A common classification of drought identifies three major types: (a) meteorological drought, due to a precipitation deficit compared to the climatology; (b) soil moisture drought, quantifying the deficit in plant water availability and the consequent reduction in agricultural production; and (c) hydrological drought, defined as a deficit in streamflow or groundwater causing, for example, reductions in water supply, hydropower production and inland water transportation.

Even within the sub-class of hydrological drought, it is possible to focus on different aspects of the phenomenon by considering different hydrological quantities, such as streamflow, groundwater level and reservoir storage volume, and the outcome of a drought analysis may differ substantially by focusing on different variables. For instance, Tallaksen and van Lanen (2004) highlighted how streamflow has a much more rapid response to meteorological drought than groundwater, and streamflow proved to be a good descriptor for operational monitoring of hydrological drought. Since the focus of this paper is on the use of river discharge

CONTACT Carmelo Cammalleri carmelo.cammalleri@ec.europa.eu

data for drought monitoring, the terms hydrological and streamflow drought are here used interchangeably. Unfortunately, even in this narrow definition of streamflow drought, the choice of a suitable drought descriptor is often subordinated to the specific purpose of the study and data availability.

In spite of the lack of a unique standard definition of hydrological (or streamflow) drought, there are some common objective features in the approaches adopted in the literature for deriving drought characteristics from streamflow records (Hisdal *et al.* 2004). Analyses are usually focused on identifying the low-flow regime of a river, by focusing on discharge values below a defined streamflow threshold and deriving water deficit characteristics that are able to characterize different traits of the drought events.

A very informative tool to characterize the entire regime of water discharge (Q) in a river, including the low flows, is the flow duration curve (FDC) (Smakhtin 2001). A FDC is constituted by representing the cumulative distribution frequency of all the flow values in decreasing order of magnitude, usually starting from an analysis of daily flow time series. The entire section of the FDC below the 50th percentile (Q_{50}) can be considered the "low-flow section", which can be interpreted as an indicator of the contribution of groundwater and subsurface flows to streamflow (Smakhtin 2001). Of course, the streamflow at the 50th percentile is a conservative upper bound to low-flow hydrology, with the absolute minimum flow representing the lower bound.

In streamflow drought analyses, a certain percentile (50th or higher) in the low-flow section of the FDC is commonly used as a boundary between normal and unusually low discharge values (Fleig *et al.* 2006). The selection of an appropriate threshold is usually dictated by the relevant water demand users and water resource practices (i.e. minimum ecological flow, power plants or water supply); overall, low-flow thresholds usually adopted in drought studies range between the 70th and 95th percentiles (Hisdal *et al.* 2004, Corzo Perez *et al.* 2011), even if lower percentiles (i.e. Q_5 or Q_{20}) have been chosen in ephemeral intermittent streams (Woo and Tarhule 1994, Tate and Freeman 2000).

Additionally, both fixed and variable (seasonal, monthly or daily) thresholds are commonly adopted, depending mainly on the goal of the analysis and the flow regime of the river (Stahl 2001); in fact, streamflow regimes are characterized by various seasonalities depending on the specific hydroclimatic region, and they may need to distinguish between summer and winter droughts, which can be done by selecting different threshold values for each season or by post-classifying the events based on the time of occurrence (Fleig *et al.* 2006).

Independently of the approach adopted to define a certain threshold for low-flow detection, a proper low-flow drought indicator needs to provide information about the duration and severity of a continuous period of low flow that is not accounted for directly in the FDC or quantiles. Indeed, rivers with similar FDCs (hence similar percentile values) may have rather distinct sequences of low-flow events due to the different sequence of discharge values in the time series (Smakhtin 2001). The defined threshold can be used within the context of the theory of runs (Yevjevich 1967) to identify all the periods (runs) when daily discharge remains below the threshold, and the partial duration series obtained can be characterized, according to the theory of runs, by three main low-flow characteristics (Smakhtin 2001): (a) the run duration, (b) the total deficit, and (c) the average intensity (as the ratio between total deficit and duration). Each of these characteristics has been used to analyse the "severity" of specific events, usually by means of a statistical analysis of all the events and by assigning a return period. Various theoretical probability distributions have been successfully adopted to fit these metrics in different study cases, including gamma, Pareto, Weibull, log-logistic and exponential distributions (Zelenhasić and Salvai 1987, Kendall and Dracup 1992, Mathier *et al.* 1992, Fleig *et al.* 2006, Mohan and Sahoo 2008).

Although numerous studies have focused on the frequency distribution of streamflow drought events over various regions (e.g. Kjeldsen *et al.* 2000, Tallaksen 2000, Shiau and Shen 2001, Modarres and Sarhadi 2010, Wu *et al.* 2015), the only indicator currently deployed for operational monitoring of hydrological drought occurrence is the standardized runoff index (SRI, Shukla and Wood 2008), which is loosely based on the methodology for calculating the standardized precipitation index (SPI, McKee *et al.* 1993). However, the SRI does not directly account for the key difference between runoff (continuous variable) and precipitation (discrete variable), since it is calculated on predetermined integration periods (e.g. monthly, 3 months); this assumption can be a significant drawback, especially in near real-time monitoring at continental scale (such as the pan-European domain).

Due to the large range of possible combinations of criteria for the development of a drought indicator based on streamflow data, the main goal of this paper is to propose a low-flow index that is both appropriate for a relatively large range of hydroclimatic conditions and implementable into an operational drought

monitoring system such as the EDO. The target spatial scale (continental Europe) and the operational nature of the EDO system require the adoption of a low-flow index that synthesizes the severity of the discharge deficit in a single quantity, and that is flexible enough to perform reasonably well on a vast range of river basin sizes.

2 Method

The first step in the development of a low-flow index is to define a threshold, starting from the analysis of the FDC, to discriminate the low-flow regime. Aimed at capturing the drought events occurring in both perennial and intermittent streams, as well as events that may occur during both dry and wet seasons, a daily threshold, $Q_{X,t}$, was adopted, where t represents the day of the year (1–365) and X the Xth percentile. This approach, similarly to the SPI, aims to characterize the "natural" low-flow regime of the river, accounting for possible seasonality in the streamflow values.

In this study, threshold values were computed on a daily basis using a streamflow dataset of 31 × n data points (with n equal to the number of years in the fitting dataset) for each day; the 31 values for a specific day, t, were obtained using a 31-day moving window centred on t (van Loon *et al.* 2010). The streamflow value corresponding to the 95th percentile ($Q_{95,t}$) of the partial daily FDC, S_t, was chosen as the daily threshold, and it can be formally defined as:

$$Q_{95,t} = \inf\left\{S_t : F_{(S_t)} \geq 0.95\right\} \quad \text{with} \quad S_t = \cup_{y=1}^{n} \cup_{j=t-15}^{t+15} Q_{y,j} \tag{1}$$

where $Q_{y,j}$ is the streamflow on the jth day of the yth year. The threshold dataset created in this way was constituted for each cell by 365 daily values (29 February values of the leap years were excluded). Two other percentiles were also considered in the analysis, the 84th and the 99th, and the reasoning behind the choice of the 95th percentile as the adopted threshold is discussed after comparing the three cases.

Having defined the daily threshold values, an event/run is defined as a period of consecutive days with $Q_t < Q_{95,t}$ (see Fig. 1), and the total deficit of the ith event, D_i, computed as:

$$D_i = \sum_{t=t_{s,i}}^{t_{e,i}} Q_{95,t} - Q_t \tag{2}$$

where $t_{s,i}$ and $t_{e,i}$ are the initial and final time steps of the run, respectively. The corresponding drought duration, d_i, is computed as $t_{e,i} - t_{s,i} + 1$. Note that the dependence of Q on the year is omitted from here on for the sake of simplicity ($Q_t \equiv Q_{y,t}$). The use of the total deficit as the sole descriptor of drought severity is dictated by its higher information content compared to the simple duration, as well as by the need in an operational system to focus on a single synthetic indicator, which can easily be examined by the users, rather than multiple information types.

Separate events that are relatively close in time may be considered mutually dependent, hence a pooling of such events is advisable. Here the data were pooled according to the inter-event time method introduced by Zelenhasić and Salvai (1987), which defines a minimum gap period, t_c, and assumes that if the inter-event time ($t_{s,i+1} - t_{e,i}$) < t_c the consecutive events are

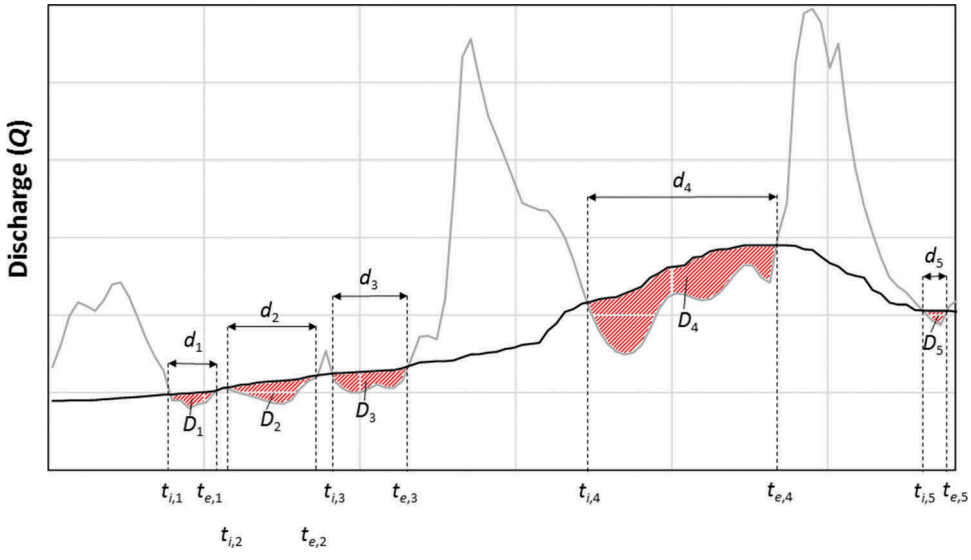

Figure 1. Schematic representation of a sequence of runs with examples of total deficit, duration, mutually dependent events and minor events. Discharge (Q) is shown as a grey line and the low-flow threshold (Q_{95}) as a black line.

considered mutually dependent and merged. In this case, the total deficit volume is the sum of the single D_i values, and the event duration is the so-called real drought duration (sum of the single event duration without the excess period). Zelenhasić and Salvai (1987) suggested a value of 6 days for t_c, whereas Tallaksen *et al.* (1997) recommended t_c = 5 days. A sensitivity analysis performed by Fleig *et al.* (2006) on seven rivers showed a sort of plateau in the pooling around t_c equal to 10 days in most streams, even if different optimal pooling values can be obtained for watersheds with strong flashy discharge or intermittent behaviour. Considering the self-imposed constraint to update the EDO monitoring system operationally every dekad (3 times per month, days 1–10, 11–20 and 21 to the end of the month), the idea of adopting a constant value of t_c = 10 days to roughly align t_c with the EDO revising time step seems reasonable within this operational context.

From an operational standpoint, it is advisable to remove the minor events on the basis of the total duration, as generated by discharge values very close to the threshold; according to the simple procedure suggested by Jakubowski and Radczuk (2004), an event shorter than a given minimum value, d_c, can be excluded from the statistical analysis of drought total deficit. As a rule of thumb, Corzo Perez *et al.* (2011) adopted a minimum duration of 3 days (10% of a month); here a value of d_c = 5 days is adopted, assuming that an event is negligible if smaller than half of the dekadal time step. Similarly to t_c, it seems reasonable to assume that all the events that start and end within a revisiting time step are of no interest for an operational monitoring system with an updating frequency of 10 days. The exclusion of all the minor events also has the double aim of improving the robustness of the successive statistical fitting and reducing the occurrence of "alarms" for very small events.

A schematic representation of the main characteristics of the runs is depicted in Figure 1; in this example, the first three runs are pooled into a single event, since both $(t_{s,2} - t_{e,1})$ and $(t_{s,3} - t_{e,2})$ are smaller than t_c, whereas the fifth event is removed for the partial duration series given that $d_5 < d_c$. The final run series includes two events, with total deficits equal to $(D_1 + D_2 + D_3)$ and D_4.

The partial duration series of the total deficit can be analysed in terms of continuous non-negative random variables generated by a time-dependent Poisson process. Due to the possibly variable characteristics of events occurring during different seasons (e.g. summer and winter events), it may be necessary to split the dataset into "homogeneous" sub-samples in order to get a satisfactory fitting. However, we assumed that thanks to the use of a daily changing threshold, as well as of a high percentile, all the observed events for a site could be analysed as part of a unique population, hence a single fit of the data can be performed.

Specifically, a simple exponential distribution is proposed here to statistically describe the total streamflow deficit values, $D = \{D_1, D_2, D_i, \ldots, D_m\}$, with a cumulative distribution function (CDF) of:

$$F(D_i;\lambda) = 1 - e^{-\lambda D_i} \quad \text{with} \quad D_i \geq 0 \tag{3}$$

where $\lambda > 0$ is the inverse scale parameter, which is equal to the inverse of the sample mean according to the maximum likelihood method. The gamma distribution, as a two-parameter generalization of the exponential distribution, was tested as an alternative option for statistical inference of D. The fitting of the two theoretical distributions was performed only if more than five events were observed on the historical dataset ($m > 5$, as adopted in most statistical tests) and the goodness of fit of the exponential and gamma distributions on the sample data was verified by means of the Kolmogorov-Smirnov statistic, as suggested in the test proposed by Lilliefors (1969). In this test, the values of the Kolmogorov-Smirnov statistic are compared against critical values (at a significance level $p = 0.05$) obtained by a Monte Carlo simulation. The use of the Kolmogorov-Smirnov statistic, rather than the chi-square or the Mann-Whitney tests, is better suited for small sample sizes, as expected for exceptional events such as droughts.

The CDF of the total water deficit represents the probability of observing values less than or equal to D_i; this quantity (ranging between 0 and 1) can be used as a direct standardized measure of the "severity" of a given deficit, constituting the proposed low-flow drought index. If the approach is applied on historical data, an event is fully defined (i.e. known starting and ending dates); hence its severity can be directly inferred through Equation (3). In an operational near real-time fashion the total deficit is computed daily (D_t) and the corresponding frequency $F(D_t;\lambda)$ is regularly revised at every system update time step (i.e. dekad) until the event is completed ($D_t \equiv D_i$), giving dynamic information on the status of the current drought. A schematic description of this implementation of the index into an operational monitoring system is provided in the flowchart in Figure 2.

The three main quantities that have to be computed daily for the low-flow index estimation are the total water deficit, D_t, the event duration, d_t, and the gap between events, g_t. These three quantities have to be initialized once at the beginning of the simulation period ($t = 0$), as $D_0 = d_0 = 0$ and $g_0 = \infty$. The flowchart in Figure 2 describes how (for $t > 0$) the daily output of the

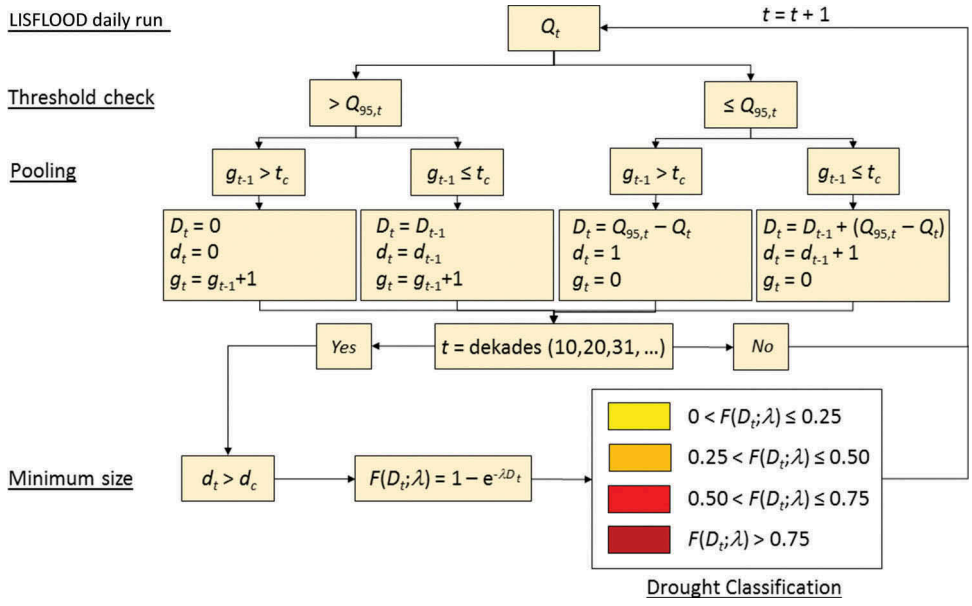

Figure 2. Flowchart describing the computational scheme for the implementation of the proposed low-flow index into an operational monitoring system. The variables $Q_{95,t}$ and λ are derived from the historical baseline dataset as described in the text, and the initial conditions are defined as $D_0 = d_0 = 0$ and $g_0 = \infty$.

LISFLOOD run (Q_t) is compared, in a first-step (*Threshold check*), against the threshold value for that specific day ($Q_{95,t}$) in order to decide whether the day can be considered to be during a drought ($Q_t \leq Q_{95,t}$) or not ($Q_t > Q_{95,t}$). In the first case (drought day, on the right wing of the flowchart), a second-step test (*Pooling*) verifies whether the day is a new drought event ($g_{t-1} > t_c$) or is part of an on-going event; in the second case (no-drought day, left wing of the flowchart), the algorithm verifies whether the gap from a previous drought event is small enough to justify a possible future pooling ($g_{t-1} \leq t_c$) or whether a future event has to be considered a new one. Depending on the results of the *Threshold check* and *Pooling* procedures, new values of D_t, d_t and g_t are computed for the tth day. If day t corresponds to the end of a dekad (10th, 20th or end-day of a month), the index $F(D_t;\lambda)$ (from here on referred to as F_D) value is computed only if the *Minimum size* condition is verified ($d_t > d_c$) and mapped as a drought event. For operational convenience, the decadal F_D values obtained are classified into four drought classes based on commonly used quantiles: mild drought: $0 < F_D \leq 0.25$; moderate drought: $0.25 < F_D \leq 0.50$: severe drought, $0.50 < F_D \leq 0.75$; and extreme drought: $F_D > 0.75$.

3 Materials

3.1 Model description

The LISFLOOD distributed hydrological rainfall–runoff model (de Roo *et al.* 2000), combined with a routing module, was used here to simulate daily discharge in the river channels. This model, developed by the floods research group of the JRC (Joint Research Centre) of the European Commission, is designed to reproduce the hydrology of large and trans-national European river catchments and it currently runs operationally within the European Flood Awareness System (EFAS; Thielen *et al.* 2009).

LISFLOOD simulates the main hydrological processes occurring in the land–atmosphere system through conceptual approaches, including infiltration of effective precipitation, soil evaporation and plant transpiration, deep percolation and groundwater recharge, whereas surface runoff routing in the river network is simulated using a 4-point implicit finite-difference solution of the kinematic wave (Chow *et al.* 1988). The model has been extensively tested in the past on a variety of hydroclimatic regions and water basins across the world (e.g. Feyen *et al.* 2007, Thiemig *et al.* 2010; Xingguo *et al.* 2006, Alfieri *et al.* 2013, 2014).

At the European scale, the EFAS operational LISFLOOD model adopts a number of static inputs developed for spatially consistent applications, including: soil hydraulic properties mapped according to the European Soil Database (http://eusoils.jrc.ec.europa.eu/ESDB_Archive/ESDBv2/index.htm) and the HYPRES dataset (Wösten *et al.* 1999); land-surface coverage and vegetation classes information derived from the CORINE land-use database (Batista e Silva *et al.* 2013); and a climatological leaf area index (LAI) dataset derived from the MODIS (Moderate-Resolution

Imaging Spectroradiometer) standard product (Myneni *et al.* 2002). The hierarchically structured river network and drainage areas were derived from a consistent digital elevation model (DEM) with 100-m grid cell resolution as part of the JRC Catchment Characterisation and Modelling (CCM) project (http://ccm.jrc.ec.europa.eu/, Vogt *et al.* 2003, Colombo *et al.* 2007, Vogt *et al.* 2007). Further details on the main LISFLOOD inputs and parameterization can be found in van der Knijff *et al.* (2010).

The set-up of the LISFLOOD model included calibration of simulated discharge against observed data, performed according to the particle swarm optimization algorithm (Zambrano-Bigarini and Rojas 2013). Daily discharge from 693 gauge stations spread across Europe were used to calibrate nine model parameters (Zajac *et al.* 2013); the calibration datasets had a minimum of 8 years of data in the period 1990–2012. A standard set of parameters was used in the fraction of the domain for which no gauge stations were available.

3.2 Dynamic inputs and simulation

For this study, daily discharge time series on a 5 km × 5 km gridded domain were produced using the calibrated LISFLOOD configuration for the period 1990–2013; however, only the data from the last 19 years (starting from 1 January 1995) were used in the model statistical fitting to limit the impact of an imperfect initialization of the model, and because of the limited number of meteorological stations in the first part of the simulation period. The length of the time series, even if limited, is close to the lower bound commonly adopted to characterize the present climate in SPI studies (20–30 years).

Additionally, the operational outputs of LISFLOOD for 2015 were also used to test the model reliability in a simulated near real-time application. The model was forced with a meteorological dataset produced within the EFAS development (Ntegeka *et al.* 2013). This dataset combines different point-scale data sources, including: the EU-FLOOD-GIS database; the JRC-MARS database, which integrates both data from national meteorological services and data acquired via the Global Telecommunication System (GTS); the World Meteorological Organization (WMO) synoptic observations; and the German Weather Service. On average, ground data collected from about 2500 precipitation and 2000 temperature stations were interpolated to derive gridded input maps (Ntegeka *et al.* 2013). This dataset is preferred over other available gridded datasets due to the high density of the combined network of stations.

4 Results and discussion

4.1 Model set-up and statistical fitting

Time series of the 95th percentile were derived for each cell of the LISFLOOD daily dataset using the 1995–2013 historical dataset. The plots in Figure 3 represent two examples of time series of $Q_{95,t}$, as well as daily discharge Q_t, for the Imera Meridionale river in Sicily (Italy), just north of the city of Licata (13.9265E, 37.1618N) and the Upper Danube river

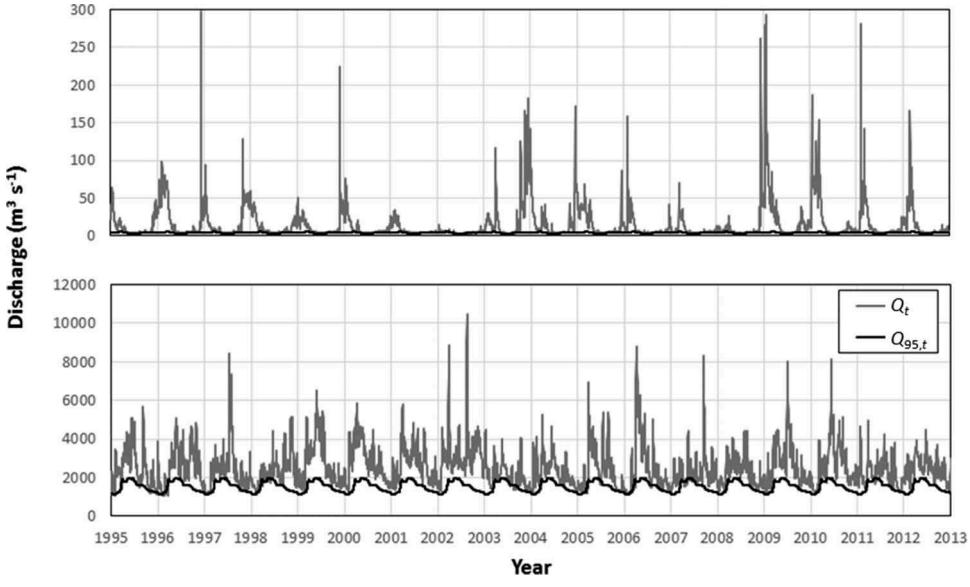

Figure 3. Example of time series of daily discharge (grey line) and low-flow threshold (black lines) for two rivers: Imera Meridionale (13.9265E, 37.1618N; upper panel) and Upper Danube (18.8866E, 47.2040N; lower panel).

just north of Budapest (18.8866E, 47.2040N). The first river has a drainage basin of about 2000 km^2 and an intermittent regime, whereas the Upper Danube has a much larger drainage basin (around 190 000 km^2 at the considered section) and a permanent streamflow. Those plots clearly show the almost constant low-flow regime in the Imera Meridionale (upper panel) which contrasts with the clear seasonality in the Upper Danube (lower panel), highlighting the ability of a daily threshold to capture both streamflow regimes.

Starting from these thresholds, partial duration series of total deficit were derived according to the approach described. Even if the total deficit time series can be computed for all the cells in the domain, the successive analyses are focused only on river cells with at least 1000 km^2 drainage area; this choice allows removal of the cells with very small streamflow, which are of limited interest for hydrological drought studies. Table 1 summarizes some European average characteristics of the time series, and includes the same statistics for the 84th and 99th percentile thresholds, in order to have two benchmark conditions.

Table 1. Summary of the European average characteristics of the total deficit partial duration series for the period 1995–2013.

Threshold	Average number of events	Average length (days)	Number of cells with >5 events[1]	No-fit cells[2] (%)
84th	36.5 ± 9.7	28.4 ± 11.2	23 948	2.2
95th	16.1 ± 4.2	17.3 ± 5.0	23 807	2.8
99th	6.8 ± 1.6	9.1 ± 2.5	6 914	71.8

[1]The total number of cells with a drainage area of at least 1000 km^2 is 24 490.
[2]Fraction of the total cells with fewer than five events.

The results in Table 1 highlight, on one hand, that limiting the minimum number of events to five for the successive fitting excludes from the analysis (No-fit) a small fraction of cells (2.8%) if the 95th percentile is adopted, which is not significantly reduced if the 84th percentile is adopted, while a significantly higher number of cells are excluded from the 99th percentile (this latter result is mainly due to the limited extension of the time series, <20 years). On the other hand, it is clear that the use of the 84th percentile as the threshold for low-flow returns a very high number of events, with an average duration close to 1 month. From this analysis, it is clear that the 95th percentile is a good compromise choice for limiting the analysis only to the most critical events that can be considered actual drought (which have on average a return period of >1 year) without excluding a large fraction of the domain from the analysis (low fraction of No-fit cells).

A more detailed analysis on the spatial distribution of the average characteristics of the runs (with the 95th percentile) was performed by means of the maps shown in Figure 4. These maps show no clear patterns, with some notable exceptions in the high number of events in the Iberian Peninsula, Poland and Macedonia, and longer events (on average) in Germany and northern Italy. These two different behaviours can be associated with shorter (but more frequent) dry periods in the former cases in contrast to longer-lasting low-flow periods in the latter. Due to the fact that the total number of days is imposed by the

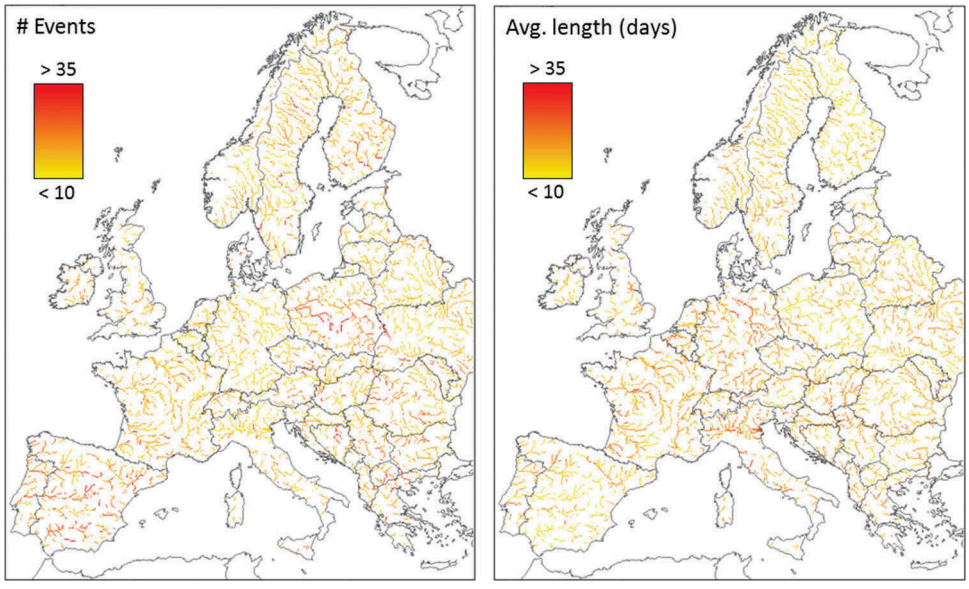

Figure 4. Spatial distribution of the number of events (left panel) and average length of the runs (right panel) in the period 1995–2013.

choice of the threshold quantile, it is clear that specular behaviour can be observed in the two maps.

The results of the Lilliefors goodness-of-fit analysis show that 20 217 cells have a significance level $p > 0.05$, representing 83% of the cells with more than five historical events. The results of the tests on the gamma distribution return a similar output, with roughly 84% of the cells with $p > 0.05$. However, seeing the exponential distribution as a special case of the gamma distribution (with just one unknown parameter), the former was chosen as the more parsimonious approach.

Overall, the results highlight the good performance of the exponential distribution in capturing the probabilistic structure of the total deficit, in spite of its simple formulation and the single parameter. Additionally, these results confirm the assumption that all the events can be considered as part of the same population, and that no sub-division of the population into sub-samples (e.g. summer and winter events) is required for a satisfactory fit. Following these considerations, the probability function expressed by Equation (3) can be considered a reliable standardization of the severity of the total streamflow deficit for the specific site.

4.2 Performance evaluation on historical case studies

A proper validation of the methodology, especially in terms of ability to monitor the occurrence of hydrological drought events in near real time, is not an easy task, mainly due to the obvious lack of actual measurements of drought severity. A qualitative evaluation of the performance of the proposed low-flow index can be made on the basis of some past events described in detail in the European Drought Reference (EDR) database (http://www.geo.uio.no/edc/droughtdb/edr/DroughtEvents.php). This database, compiled within the framework of the EU funded DROUGHT R&SPI Project (http://www.eu-drought.org/), aims to concentrate in a single location a large set of information on historical drought events across Europe.

Focusing on hydrological droughts that occurred in the period of interest (1995–2015), two main drought periods were recognized in the database: the Northern European drought in 1995–1997 and the East/Southeast European drought in 2000. In detail, in the UK and Ireland a summer (July–September) decline in river flow was observed in 1995 due to hot dry conditions. This event is generally considered part of a longer drought that occurred between 1995 and 1997. In other Northern European countries, such as Germany, the Netherlands, Belgium and the Scandinavian Peninsula countries, a severe reduction in runoff was observed around March–October 1996. During spring and summer of 2000, drought conditions were reported in several Eastern European countries: many impacts were related to crop production, and Croatia reported problems in fresh water fisheries, hydropower production and tourism as well as dried up streams and wells.

Starting from the information stored in this database, four study cases, corresponding to the same number of rivers, were selected to evaluate the performance of the proposed indicator in a simulated near real-time monitoring system. The low-flow index in Equation (3) was computed on the total deficit values updated every dekad (as schematized in Fig. 2) during the period surrounding the drought events recognized in the EDR database. The four study rivers were (1) the Shannon in Ireland (the longest river of the island), (2) the Weser in northwest Germany (the longest river to reach the sea entirely within German territory), (3) the Österdal in southeast Sweden (a 300-km-long river, converging into the Dalälven River), and (4) the Sava crossing former-Yugoslavia countries (one of the main tributaries of the Danube).

Figure 5 presents the temporal evolution of F_D in the four study cases, with the colour code associated with the drought classes (as described in Fig. 2). The years depicted for each site were adapted to the period of the specific drought, and a single block in the upper row shows the F_D class for a dekad. As an additional benchmark to test the performance of the proposed index, the monthly SRI values were also computed on the basis of the procedure described in Shukla and Wood (2008), with the fitting of the gamma CDF replaced by the empirical cumulative distribution function. In order to represent the data in a colour scheme analogous to the one adopted for the F_D, the SRI values were classified according to the SPI classification of McKee *et al.* (1993) as modified in Agnew (2000) (see Fig. 5 caption).

Overall, the F_D time series in Figure 5 show good capability of the proposed low-flow indicator to capture the occurrence of the main events described in the EDR database. For the Shannon River it is possible to observe two main events: the first between July and October 1995 and the second in early 1997. Those two events correspond to the decline in water flow observed in Ireland and the southern UK during the long drought of 1995–1997. In both the Weser and the Österdal rivers several dekades with severe and extreme drought conditions can be observed during the first nine months of 1996, which is in good agreement with the EDR reports. Some other minor events can

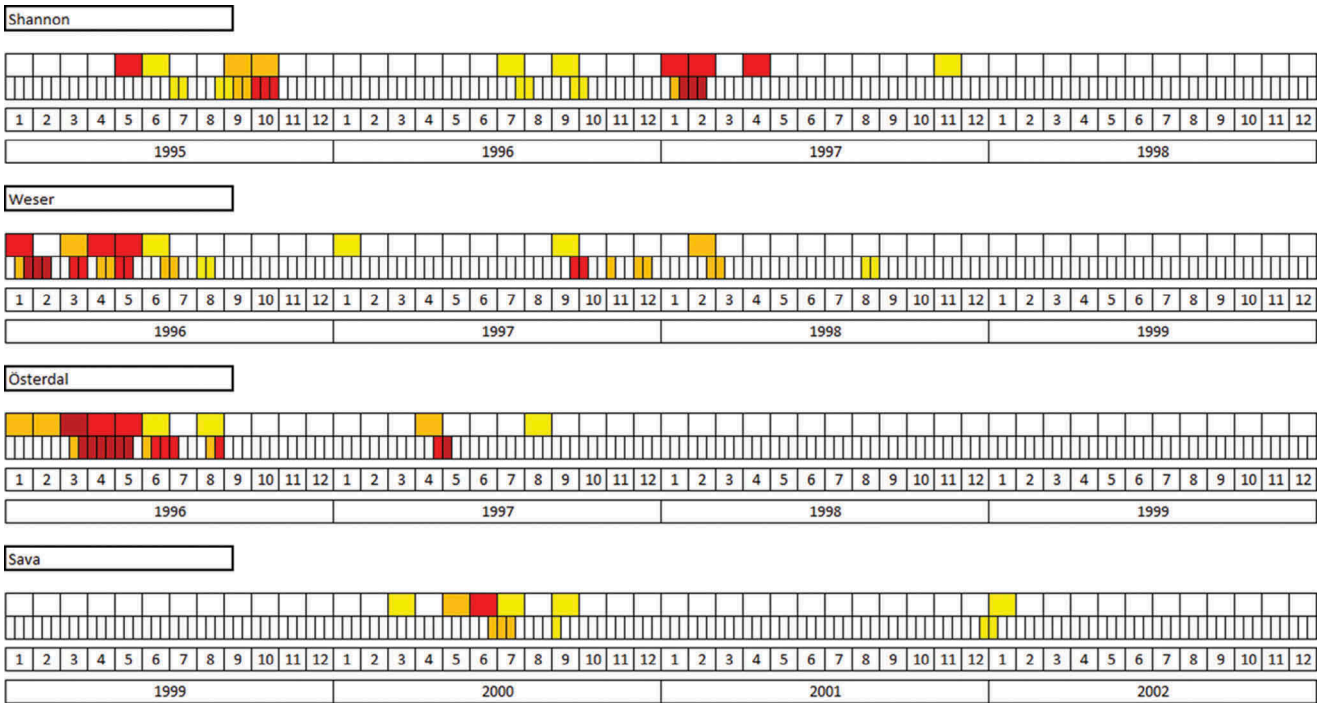

Figure 5. Four examples of near real-time monitoring of hydrological drought with the SRI (upper line) and the proposed index (lower line). Each SRI time series represents the monthly values classified as follows: −0.84 to −1.00: yellow, −1.01 to −1.50: orange, −1.51 to −2.00: red, <−2.00: maroon (see Agnew 2000); the F_D time series are the dekadal values classified with the following colour scheme: mild: yellow, moderate: orange, severe: red, extreme: maroon (see Fig. 2).

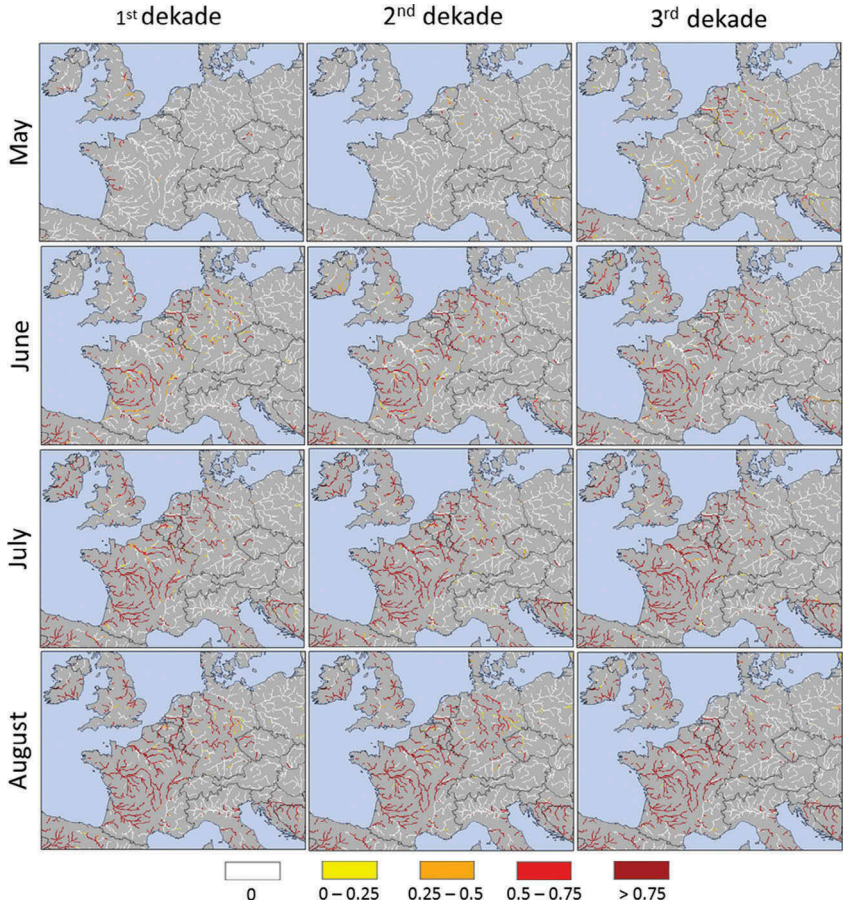

Figure 6. Sequence of F_D dekadal maps for summer (May–August) 2015 in Central Europe. The land cells with drainage area <1000 km^2 are depicted in grey; the main rivers are coloured according to the scheme: no-drought: white, mild: yellow, moderate: orange, severe: red, extreme: maroon (see Fig. 2).

be also observed in late 1997 for the Weser and early 1997 for the Österdal; these events coincide with drought impacts on hydropower production and navigation reported for the Netherlands, Belgium and the Scandinavian countries. Finally, a moderate drought event is reproduced in the Sava River during the summer of 2000; this event, even if not as marked as the others, captures the timing (i.e. June–July) reported in the EDR database.

The intercomparison of F_D with the monthly SRI highlights good correspondence in the events detected by the two methods, which is not surprising given that both of them are based on the same source of streamflow data (LISFLOOD). However, in some circumstances it is possible to perceive an advantage of the proposed index compared to that based on pre-determined integration windows (calendar month in this specific case). For the case of the Shannon River, for example, the SRI detects two consecutive months with moderate (severe) drought in September–October 1995 (January–February 1997), but it is not able to account for the fact that, since the two consecutive anomalies are actually part of the same drought event, the streamflow values should be cumulated to account for gradually increasing severity. This behaviour demonstrates the benefit of an approach that detects the start and the continuity of an event on the basis of upcoming new data, fully exploiting the daily temporal resolution.

4.3 Analysis of a near real-time case study over central Europe

As a final test of the index, its ability to capture the most recent drought event observed over Central Europe was verified by plotting the spatial distribution of the F_D index during summer (May–August) 2015 (Fig. 6). These maps were generated using the daily outputs of the LISFLOOD model produced in near real time with the EFAS system. From July 2015, an intense heatwave spread through Western and Central Europe (Portugal, Spain, France and Germany), which was also accompanied by unusually low rainfall in both France and Germany, as highly documented by the news media (e.g. http://www.weather.com/forecast/news/europe-heat-wave-record-highs-june-july-2015). According to the information provided by the German Weather Service (DWD (Deutscher Wetterdienst) 2015), central Germany was severely affected in June and July, whereas northeast and southern Germany experienced higher than usual precipitation. Contextually, water restrictions were enacted in both July and August in most of western and northeast France (MEDDE – MAAF 2015).

The dekadal maps in Figure 6 depict the spatiotemporal evolution of the drought quite well, with almost no drought cells in May, arising drought conditions in western France and northwest Germany in June, and the spread of the phenomenon in July and August. It is worth noting that most of southern and northeast Germany remained unaffected by the drought, as a consequence of localized thunderstorms that occurred in July (DWD 2015). According to these F_D maps, most of France was affected by drought in July–August, with the Provence region the only exception; this spatial distribution is in good agreement with the areas where water restrictions were in force during that period.

5 Summary and conclusions

The main goal of this paper was to propose and test an operational tool for hydrological drought monitoring within the EDO system. The index exploits the daily discharge data available in near real-time over the pan-European domain through the LISFLOOD model developed by the JRC of the European Commission. Following the theory of runs (Yevjevich 1967), a daily 95th percentile threshold level (based on a 31-day moving window) was used to extract a partial time series of total water deficit values; the use of a daily threshold approach showed the ability to deal with a large range of hydroclimatic regimes, including both intermittent and perennial rivers, whereas the 95th percentile allowed a reasonable number of events (on average over the full domain) to be obtained without limiting detection to only the most extreme events. The length of the available time series (almost 20 years) played a key role in selecting the 95th percentile rather than higher ones (e.g. 99th), hence further refinement of this value may be made when a longer dataset becomes available.

The proposed hydrological drought indicator is based on the cumulative distribution function value of the total streamflow deficit, which was successfully fitted through a simple exponential distribution over most of the domain. Pooling of mutually dependent successive events and negligibility of the minor ones is accounted for by means of a simple spatial-invariant parameterization derived from the relevant literature. A more refined tuning of these parameters can be performed on a watershed basis, especially for the pooling, but the available literature on the topic does not support a current operational implementation.

The proposed approach allows near real-time monitoring of the evolution of a drought event by quantifying the cumulative deficit up to the update time. This

proposed dynamic approach accounts for the continuous nature of streamflow data and exploits the availability of daily flow data without recourse to a predetermined temporally aggregated time window (i.e. monthly runoff data in the SRI). In contrast to the commonly adopted "anomalies" approach (i.e. SPI, SRI), this method better reproduces the conceptual mechanism behind the evolution of a drought event as a phenomenon that is derived from a continuous hydrological quantity with daily values that are strongly dependent on the antecedent status.

The ability of the proposed low-flow indicator to capture the occurrence of hydrological drought events was tested against some well-known historical case studies, which were selected from the European Drought Reference (EDR) database as having documented impacts on streamflow levels, hydropower production and river ecosystems. This analysis was an attempt to understand the role of this tool in detecting the start of a low-flow period, as well as the duration of the affected period, in a similar fashion to a near real-time monitoring system. The ability to infer the most recent drought event that occurred in Central Europe during summer 2015 was also verified.

The temporal evolution of F_D during the test drought events seems to be well reproduced by the model, with good correspondence with the documented duration of the events, the period of occurrence and the starting time. It also shows several common features with the temporal dynamics of the monthly SRI (thanks to the use of the same source for streamflow data), even if the advantage of not relying on predetermined fixed integration windows (i.e. calendar month) is evident in the ability to quantify the total magnitude of the longer events.

Also, the spatial evolution of the summer 2015 drought is well captured according to the information on impacted areas as disseminated by the local weather services. Even if no analyses on the actual magnitude of the drought can be made on the basis of the data available in the EDR database or in the news, the proposed low-flow index seems suitable as an operational tool for near real-time monitoring of the evolution of hydrological drought events across Europe. On the basis of the results obtained, the adoption of this index within an operational system such as EDO seems feasible, and further developments of the index, as well as fine tuning of the parameterization (i.e. spatialization of t_c), may be related to its ability to detect future events correctly within the context of actual monitoring activities.

Disclosure statement

No potential conflict of interest was reported by the authors.

Funding

This work was supported by the Joint Research Centre of the European Commission.

References

Agnew, C.T., 2000. Using the SPI to identify drought. *Drought Network News (1994–2001)*, 12 (1), 1–12: http://digitalcommons.unl.edu/droughtnetnews/1

Alfieri, L., *et al.*, 2013. GloFAS – global ensemble streamflow forecasting and flood early warning. *Hydrology and Earth Systems Sciences*, 17, 1161–1175. doi:10.5194/hess-17-1161-2013

Alfieri, L., *et al.*, 2014. Advances in pan-European flood hazard mapping. *Hydrology and Processing*, 28, 4067–4077. doi:10.1002/hyp.v28.13

Batista e Silva, F., Lavalle, C., and Koomen, E., 2013, A procedure to obtain a refined European land use/cover map. *Journal Land Use Sciences*, 8 (3), 255–283. doi:10.1080/1747423X.2012.667450

Chow, V.T., Maidment, D., and Mays, L.W., 1988. *Applied hydrology*. New York: McGraw-Hill.

Colombo, R., *et al.*, 2007, Deriving river networks and catchments at the European scale from medium resolution digital elevation data. *Catena*, 70 (3), 296–305. doi:10.1016/j.catena.2006.10.001

Corzo Perez, G.A., *et al.*, 2011. On the spatio-temporal analysis of hydrological droughts from global hydrological models. *Hydrology and Earth Systems Sciences*, 15, 2963–2978. doi:10.5194/hess-15-2963-2011

de Roo, A., Wesseling, C., and van Deursen, W., 2000. Physically based river basin modelling within a GIS: the LISFLOOD model. *Hydrology and Processing*, 14, 1981–1992. doi:10.1002/(ISSN)1099-1085

DWD (Deutscher Wetterdienst), 2015. *Pressemitteilung – The weather in Germany in July 2015* [online]. Available from: http://www.dwd.de/bvbw/generator/DWDWWW/Content/Presse/Pressemitteilungen/2015/20150730__Deutschlandwetter__Juli__2015__e,templateId=raw,property=publicationFile.pdf/20150730_Deutschlandwetter_Juli_2015_e.pdf [Accessed 17 September 2015].

European Commission, 2007. Addressing the challenge of water scarcity and droughts in the European Union, Impact Assessment SEC(2007)993, 63 Available from: http://ec.europa.eu/environment/water/quantity/pdf/comm_droughts/impact_assessment.pdf

Feyen, L., *et al.*, 2007. Parameter optimisation and uncertainty assessment for large-scale streamflow simulation with the LISFLOOD model. *Journal of Hydrology*, 332, 276–289. doi:10.1016/j.jhydrol.2006.07.004

Fleig, A.K., *et al.*, 2006. A global evaluation of streamflow drought characteristics. *Hydrology and Earth Systems Sciences*, 10, 535–552. doi:10.5194/hess-10-535-2006

Hisdal, H., *et al.*, 2004. Hydrological drought characteristics. *In*: L.M. Tallaksen and H.A.J. van Lanen, eds. *Hydrological*

Drought - Processes and estimation methods for streamflow and groundwater. Amsterdam: Elsevier Sciences B.V., 139–198.

Jakubowski, W. and Radczuk, L., 2004. Estimation of hydrological drought characteristics NIZOWKA2003 – Software Manual. *In*: L.M. Tallaksen and H.A.J. van Lanen, eds. *Hydrological Drought – Processes and estimation methods for Streamflow and groundwater*. Amsterdam: Elsevier Sciences B.V. [CD-ROM].

Kendall, D. and Dracup, J., 1992, On the generation of drought events using an alternating renewal-reward model. *Stochastic Hydrology Hydraulics*, 6 (1), 55–68. doi:10.1007/BF01581675

Kjeldsen, T.R., Lundorf, A., and Rosbjerg, D., 2000, Use of a two-component exponential distribution in partial duration modelling of hydrological droughts in Zimbabwean rivers. *Hydrological Sciences Journal*, 45 (2), 285–298. doi:10.1080/02626660009492325

Lilliefors, H.W., 1969, On the Kolmogorov-Smirnov test for the exponential distribution with mean unknown. *Journal of American Statistical Association*, 64 (325), 387–389. doi:10.1080/01621459.1969.10500983

Mathier, L., *et al*., 1992, The use of geometric and gamma-related distributions for frequency analysis of water deficit. Stochastic *Hydrology and Hydraulics*, 6 (4), 239–254. doi:10.1007/BF01581619

McKee, T.B., Doesken, N.J., and Kleist, J., 1993. The relationship of drought frequency and duration to time scales. *In*: *Proceedings of the 8th Conference of Applied Climatology*, 17–22 January 1993. Boston, MA: American Meteorological Society, 179–184.

MEDDE – MAAF (Ministère de l'Ecologie, du Développement Durable, et de l'Energie – Ministère de l'Agriculture, de l'Agroalimentaire et de la Forêt), 2015. *PROPLUVIA: La consultation des arrêtés de restriction d'eau* [online]. Available from: http://propluvia.developpement-durable.gouv.fr/propluvia/faces/index.jsp [Accessed 17 September 2015].

Modarres, R. and Sarhadi, A., 2010, Frequency distribution of extreme hydrologic drought of Southeastern semiarid region. *Iranian Journal of Hydraulic Engineering*, 15 (4), 255–264.

Mohan, S. and Sahoo, P.K., 2008. Stochastic simulation of droughts. Part 1: point droughts. *Hydrological Processing*, 22, 854–862. doi:10.1002/(ISSN)1099-1085

Myneni, R.B., *et al*., 2002. Global products of vegetation leaf are and fraction absorbed PAR from year one of MODIS data. *Remote Sensing of Environment*, 83(1–2), 214–231.

Ntegeka, V., *et al*., 2013. *EFAS-Meteo: a European daily high-resolution gridded meteorological data set for 1990–2011*. EUR - Scientific and Technical Research series. Luxembourg: Office of the European Union.

Shiau, J.-T. and Shen, H.W., 2001, Recurrence analysis of hydrologic droughts of differing severity. *Journal Water Researcher Planning Management (ASCE)*, 127 (1), 30–40. doi:10.1061/(ASCE)0733-9496(2001)127:1(30)

Shukla, S. and Wood, A.W., 2008. Use of a standardized runoff index for characterizing hydrologic drought. *Geophysics Researcher Letters*, 35, L02405. doi:10.1029/2007GL032487

Smakhtin, V.U., 2001. Low flow hydrology: a review. *Journal of Hydrology*, 240, 147–186. doi:10.1016/S0022-1694(00)00340-1

Spinoni, J., *et al*., 2015. European drought climatologies and trends based on a multi-indicator approach. *Global Planetary Change*, 127, 50–57. doi:10.1016/j.gloplacha.2015.01.012

Stahl, K., 2001. *Hydrological drought: a study across Europe*. Thesis (PhD). Albert-Ludwigs-Universität Freiburg. Available from: http://www.freidok.uni-freiburg.de/volltexte/202

Tallaksen, L.M., 2000. Streamflow drought frequency analysis. *In*: J. Vogt and F. Somma, eds. *Drought and drought mitigation in Europe*. Dordrecht: Kluwer Academic Publications, 103–117.

Tallaksen, L.M., Madsen, H., and Clausen, B., 1997, On the definition and modelling of streamflow drought duration and deficit volume. *Hydrological Sciences Journal*, 42 (1), 15–33. doi:10.1080/02626669709492003

Tallaksen, L.M. and van Lanen, H.A.J., 2004. Drought as natural hazard: Introduction. *In*: L.M. Tallaksen and H.A.J. van Lanen, eds. *Hydrological Drought - Processes and estimation methods for streamflow and groundwater*. Amsterdam: Elsevier Sciences B.V., 3–17.

Tate, E.L. and Freeman, S.N., 2000, Three modelling approaches for seasonal streamflow droughts in southern Africa; the use of a censored data. *Hydrological Sciences Journal*, 45 (1), 27–42. doi:10.1080/02626660009492304

Thielen, J., *et al*., 2009. The European Flood Alert System – Part 1: Concept and development. *Hydrology Earth System Sciences*, 13, 125–140. doi:10.5194/hess-13-125-2009

Thiemig, V., *et al*., 2010. Ensemble flood forecasting in Africa: A feasibility study in the Juba-Shabelle river basin. *Atmospheric Science Letters*, 11, 123–131. doi:10.1002/asl.266

van der Knijff, J.M., Younis, J., and de Roo, A.P.J., 2010. LISFLOOD: A GIS-based distributed model for river basin scale water balance and flood simulation. *International Journal Geographic Information Sciences*, 24, 189–212. doi:10.1080/13658810802549154

van Loon, A.F., *et al*., 2010. Understanding hydrological winter drought in Europe. *In*: E. Servat, *et al*., *Global change: facing risks and threats to water resources, proceedings of the Sixth World FRIEND conference*, October 2010 Fez 340. Wallingford: IAHS Publications, 189–197.

Vogt, J.V., Colombo, R., and Bertolo, F., 2003, Deriving drainage networks and catchment boundaries: A new methodology combining digital elevation data and environmental characteristics. *Geomorphology*, 53 (3–4), 281–298. doi:10.1016/S0169-555X(02)00319-7

Vogt, J.V., *et al*., 2007. *A pan-European river and catchment database* [online]. EUR Scientific and Technical Research series EUR 22920 EN, ISSN 1018-5593, Luxembourg, 124 p. Available from: http://ccm.jrc.ec.europa.eu/documents/CCM2-Report_EUR-22920-EN_2007_STD.pdf [Accessed 13 October 2016].

Woo, M. and Tarhule, A., 1994, Streamflow droughts of northern Nigerian rivers. *Hydrological Sciences Journal*, 39 (1), 19–34. doi:10.1080/02626669409492717

Wösten, J.H.M., *et al.*, 1999. Development and use of a database of hydraulic properties of European soils. *Geoderma*, 90, 169–185. doi:10.1016/S0016-7061(98)00132-3

Wu, Z., *et al.*, 2015. Analysis of hydrological drought frequency for the Xijiang river basin in South China using observed streamflow data. *Natural Hazards*, 77, 1655–1677. doi:10.1007/s11069-015-1668-z

Xingguo, M.O., *et al.*, 2006. Parameter conditioning and prediction uncertainties of the LISFLOOD-WB distributed hydrological model. *Hydrological Sciences Journal*, 51, 45–65. doi:10.1623/hysj.51.1.45

Yevjevich, V., 1967. *An objective approach to definitions and investigations of continental hydrological droughts*. Fort Collins: Colourado State University, Hydrology Paper 23.

Zajac, Z., *et al.*, 2013. *Calibration of the Lisflood hydrological model for Europe*. EUR - Scientific and Technical Research series. Luxembourg: Office of the European Union.

Zambrano-Bigiarini, M. and Rodrigo Rojas, R., 2013. A model-independent Particle Swarm Optimisation software for model calibration. *Environment Model Software*, 43, 5–25. doi:10.1016/j.envsoft.2013.01.004

Zelenhasić, E. and Salvai, A., 1987, A method of streamflow drought analysis. *Water Resources Researcher*, 23 (1), 156–168. doi:10.1029/WR023i001p00156